2 Basics of Microgrid Control

2.1 Microgrid Operation

Today's microgrids normally contain the following components: a localized group of electricity generators, including solar, wind, fuel cell, combined heat and power, and diesel generators; loads such as buildings, factories, and shops; and storage, which may be coordinated and managed by a microgrid energy management system (EMS) or a platform with similar functionalities (see Figure 2.1). Because of their multiple dispersed energy resources and their ability to isolate from the main grid, microgrids provide a promising paradigm for improving the resiliency of the electric distribution infrastructure.

As an illustrative example, Canada-based Alectra Utilities (formerly PowerStream) has created a small-scale microgrid demonstration project at its head office to validate the potential economic and resilience benefits to their customers. As can be seen in Figure 2.2, the Alectra microgrid consists of a solar array, a wind turbine, a natural-gas generator, a lead-acid battery, and a lithium-ion battery. The microgrid loads include the lighting, air conditioning, and refrigeration for the company's cafeteria, entrance area, and electric vehicle charging station.

A microgrid may operate in four modes: grid-connected (i.e., connected to the main grid), islanded (i.e., disconnected from the main grid), islanding (i.e., transitioning from grid-connected to islanded), or reconnected (i.e., transitioning from islanded to grid-connected). When normal conditions apply to the main grid, islanding can be conducted intentionally, but it can also be performed unintentionally when the grid is subjected to abnormal conditions (e.g., faults). In this book, we focus on microgrids with a high penetration of renewable energy resources. Though these microgrids bring significant environmental benefits, they also pose major challenges in management and control. For instance, unintentional islanding, also known as an emergency operation, is particularly challenging for such microgrids since renewable energy resources are intermittent, uncertain, and have much smaller inertias than traditional power generation plants [1, 2]. In such microgrids, it is extremely important to achieve fast voltage and frequency control in an emergency operation; otherwise, the system may lose its balance between load and generation, which could lead to eventual collapse.

Like many functionalities, rapid voltage and frequency control rely on the microgrid's communication infrastructure (see Figure 2.1b). Communication can be conducted from the microgrid's EMS to the main grid's EMS, between the microgrid's

https://doi.org/10.1017/9781108596589.004 Published online by Cambridge University Press

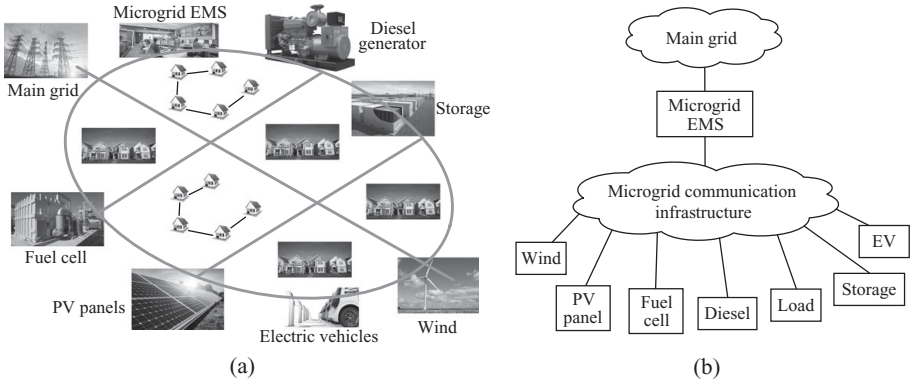

Figure 2.1 Illustration of a microgrid. (a) The various components in a microgrid. (b) Schematic view of a microgrid where the various components are connected by a communication infrastructure. Figure courtesy of Professor Bing Wang

Figure 2.2 A microgrid control room at Alectra Utilities (formerly PowerStream).

EMS and its various components, and among the various components. There are many types of communication data, from small periodic control messages to large data messages, with diverse quality of service (QoS) requirements depending on the type of data and the microgrid's mode. In the most stringent scenarios (e.g., microgrid control messages when entering the emergency operation mode), the delay requirement may be just a few milliseconds. In less stringent scenarios (e.g., during steady-state control, intentional islanding, and reconnection), the delay requirement may be as long as a few seconds. The least stringent scenarios apply to the transferral of energy management information, which can tolerate delays as long as a few minutes.

https://doi.org/10.1017/9781108596589.004 Published online by Cambridge University Press

As mentioned earlier, the networking technologies used in microgrid deployments may vary depending on a number of factors such as deployment costs, required coverage, and suitability for control. For instance, when deployment costs are not a concern, adopting dedicated networks of redundant fiber optics can provide fast and reliable communication; in areas with well-established wired infrastructures (e.g., Ethernet), adopting the existing infrastructure would be a natural choice. However, in certain rural or disaster areas, it might be too costly or infeasible to establish a wired network, making wireless technologies (e.g., WiFi, WiMax, or cellular network) the only option. No matter what networking technologies are used, the communication infrastructure must satisfy the diverse QoS requirements and be resilient to network failure (in the form of degraded performance or complete failure) caused by congestion, interference, or hardware/software faults [3]. The latter requirements demand that the communication infrastructure provide multiple network paths, through rich connectivity in network topology or multiple networking technologies (e.g., Ethernet, WiFi, WiMax, cellular networks) [4]. Because these technologies must be managed carefully to ensure that a microgrid can operate properly in the face of a network failure, a software-defined network should be used. As detailed in Chapter 4, this general communication architecture can be used in a wide range of microgrid deployments, despite the underlying networking technologies that are being adopted.

2.2 Microgrid Control

With the support of the communication infrastructure, microgrid control schemes – especially those designed for the operation of microgrids under islanded situations – can be developed. Microgrid control is particularly challenging when there is a high penetration of renewable energy resources in the microgrid. In this chapter, we focus on droop control, an important primary control strategy for rapidly restoring a microgrid's voltage and frequency. Secondary control, remedial action scheme (microRAS), and optimal power flow will also be discussed briefly.

2.2.1 Hierarchical Control Principle

The popular droop control scheme implemented in microgrids [5–16] was perhaps inspired by the droop control of synchronous generators in a traditional power system [17, 18]. In traditional, vertically integrated utilities, the power system control follows a hierarchical control framework that includes the primary control, the secondary control, and the tertiary control. Even though there has been a trend of utility restructuring and deregulation, the hierarchical control framework has been largely retained [19]. The primary control, or droop control, is at the bottom level and is achieved through the turbine governor and its speed-droop characteristic; all the control commands from the upper levels are executed at this level. The droop control is a decentralized proportional control, where only local measurements are used as feedback signals and the droop coefficient is the control gain [20].

https://doi.org/10.1017/9781108596589.004 Published online by Cambridge University Press

The secondary control is used to force the droop control to eliminate frequency deviations and maintain the agreed tie line power flows between utilities. In isolated grids, the secondary control is degenerated into the frequency control only [18]. Because the secondary control normally relies on communication networks, it is slower than the primary control. The tertiary control is slower than the secondary control, and at the EMS level, it may encompass more advanced functions such as optimal power flow (OPF) and economic dispatch [21].

In a traditional power system, one or more power plants are enrolled in the load frequency control (LFC) to maintain frequency. In general, system frequency is governed by load and generation conditions. If the load suddenly increases and becomes greater than the power generation, the frequency tends to decrease. Accordingly, the increase in load will be supplied by the kinetic energy released from the generators [22]. Once the turbine governors of all the power plants sense the frequency drop, the droop control starts to increase power generation by the required amount, resulting in an improved but reduced frequency determined by the speed-droop curves. Later, the LFC will further increase power generation in the generators registered on the LFC to bring the system frequency back to the scheduled or nominal value, which is the secondary control. Similarly, if the load suddenly decreases and becomes lower than the power generation, the excessive generation will be converted to kinetic energy, which speeds up all the generators until the frequency increase is sensed by the governors [22]. The droop control and secondary control will then be initiated to recover the frequency.

In a turbine governor system, a speed sensor (e.g., a flyball for a mechanical-hydraulic governor and a frequency transducer for an electrohydraulic governor [23]) measures the speed of the turbine and opens the steam valves on the steam turbines or the wicket gates on the hydroturbines if the speed decreases [22]. This turbine control system produces a steady-state speed-droop curve as shown in Figure 2.3. Thus, the droop control is an inherent characteristic of a turbine generator system.

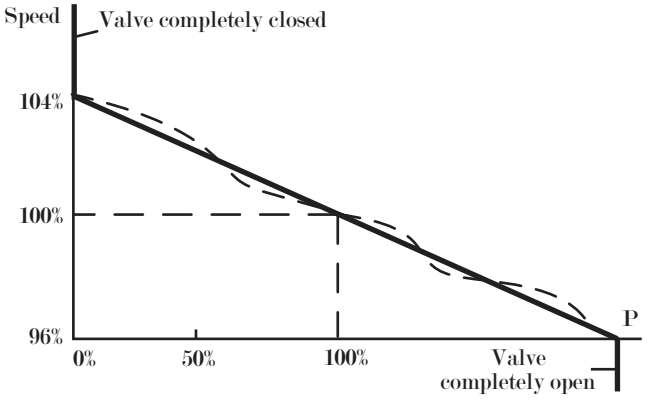

Figure 2.3 Steady-state speed droop of a synchronous generator. Figure courtesy of Dr. H. W. Dommel's lecture notes [22]

https://doi.org/10.1017/9781108596589.004 Published online by Cambridge University Press

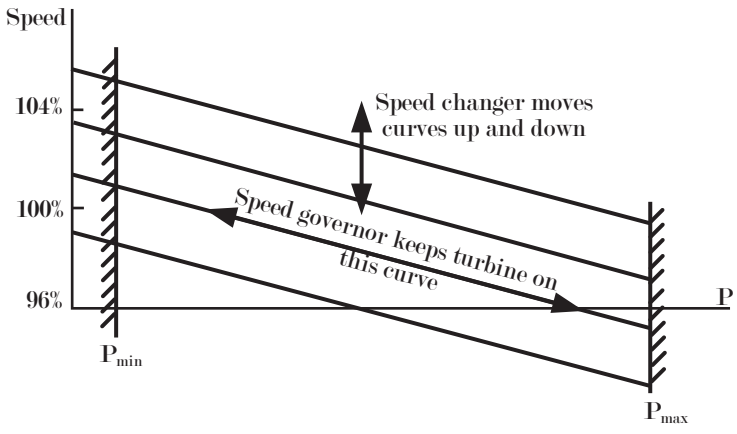

Figure 2.4 Secondary control of a synchronous generator. Figure courtesy of Dr. H. W. Dommel's lecture notes [22]

For a grid-tied synchronous generator without a secondary control device, the turbine power at the nominal speed will always be the rated power (see Figure 2.3). To change power output at will, a speed changer is equipped to change the valve's or the wicket gate's position independently of the primary control action, which can create a series of steady-state speed-droop curves as shown in Figure 2.4. Thus the power output at the nominal speed can be set to any value within $P_{\min}$ and $P_{\max}$ through the speed changer [22], which enables the secondary control for the LFC generators to fully recover the system frequency.

2.2.2 Droop Control for Microgrids

A majority of the renewable distributed energy resources (DERs) in microgrids produce direct current (DC) power (e.g., photovoltaics) or operate at a high frequency (e.g., single-shaft microturbines) or a variable frequency (e.g., wind turbine generators). Those DERs are interconnected with the alternating current (AC) microgrid backbone through inverters [24]. As a result, the droop control of inverter-dominated microgrids is deployed on DER inverters. Unlike the speed governor for a set of synchronous generators described in Subsection 2.2.1, inverters do not have any inherent tendency toward the speed-droop characteristic, meaning a droop effect must be artificially created through the inverter controller.

One possible motivation for using a conventional droop control strategy at the microgrid level is to help the main grid and its microgrids respond coherently to frequency changes, which in turn helps achieve a consistent control effect throughout the grid that can reduce concerns about microgrids' impact on grid stability and reliability [25]. In addition, droop control can be achieved without a centralized supervisory control, as it uses local variables to regulate power output. Thus, it is a modular and plug-and-play design in itself.

https://doi.org/10.1017/9781108596589.004 Published online by Cambridge University Press

Droop control can be deployed on DER inverters operating in a grid-forming mode, i.e., voltage source inverters (VSIs). Here, a grid-forming inverter means an inverter that is controlled such that its output voltage can be specified as needed [20]. To achieve droop control, a cascaded control scheme including an outer voltage loop and an inner current loop can be integrated in a VSI [20]. For one or more DERs participating in microgrid stabilization and voltage recovery, frequency-droop and voltage-droop control strategies are used to share active and reactive power among DERs. One straightforward approach to implementing droop control is to use P as a function of f and Q as a function of V, resulting in the so-called $f - P/V - Q$ control, expressed as follows:

$$P = P^* + K_f(f^* - f) \tag{2.1a}$$

$$Q = Q^* + K_V(V^* - V). \tag{2.1b}$$

Some of the literature on this subject [25] argues that measuring instantaneous real power is more viable than obtaining an accurate measurement of instantaneous frequency. This might have been a reason why a droop control with f as a function of P and V as a function of Q was proposed, where the VSI output power is measured and used to regulate its output frequency and voltage. This so-called $P - f/Q - V$ control is expressed as follows:

$$f = f^* + K_P(P^* - P) \tag{2.2a}$$

$$V = V^* + K_Q(Q^* - Q). \tag{2.2b}$$

Through the aforementioned $P - f/Q - V$ droop control, microgrid inverters are able to mimic the behavior of a synchronous generator that increases its active power output in response to a load increase and reduces its frequency, as Figure 2.3 illustrates. Here, f^* and V^* are the reference values for the microgrid's frequency and the amplitude of the inverter output voltage, respectively, and P^* and Q^* are the corresponding active and reactive power outputs. One type of typical droop control scheme deployed on a two-level three-phase inverter is illustrated in Figure 2.5.

The inner current-controlled loop determines the reference voltage waveforms for the pulse-width modulation (PWM) of the VSI [26]. The control scheme can be implemented in a synchronous $dq0$ frame through which the three-phase output currents are transformed into their direct (d-axis) and quadrature (q-axis) components i_d and i_q. The d-axis and q-axis currents pass through a low-pass filter. Then they are compared with reference signals i_{dref} and i_{qref}, which are specified by the outer voltage control loop. The error signals are applied to a proportional-integral (PI) control block with a current limiter, which determines the d- and q-components of reference voltages v_{dref} and v_{qref} after including the voltage feed-forward terms and the cross-coupling elimination terms. Eventually, the three-phase reference signals for the PWM signal generator are specified by transforming the dq quantities to abc quantities.

The outer loop realizes the $P - f/Q - V$ control purpose, where the VSI active power output is used to regulate the voltage angle through the integration of the frequency, and the VSI reactive power output is used to regulate the voltage amplitude [27]. The controller's output signals are v_{dref} and v_{qref}, which will be used to generate

https://doi.org/10.1017/9781108596589.004 Published online by Cambridge University Press

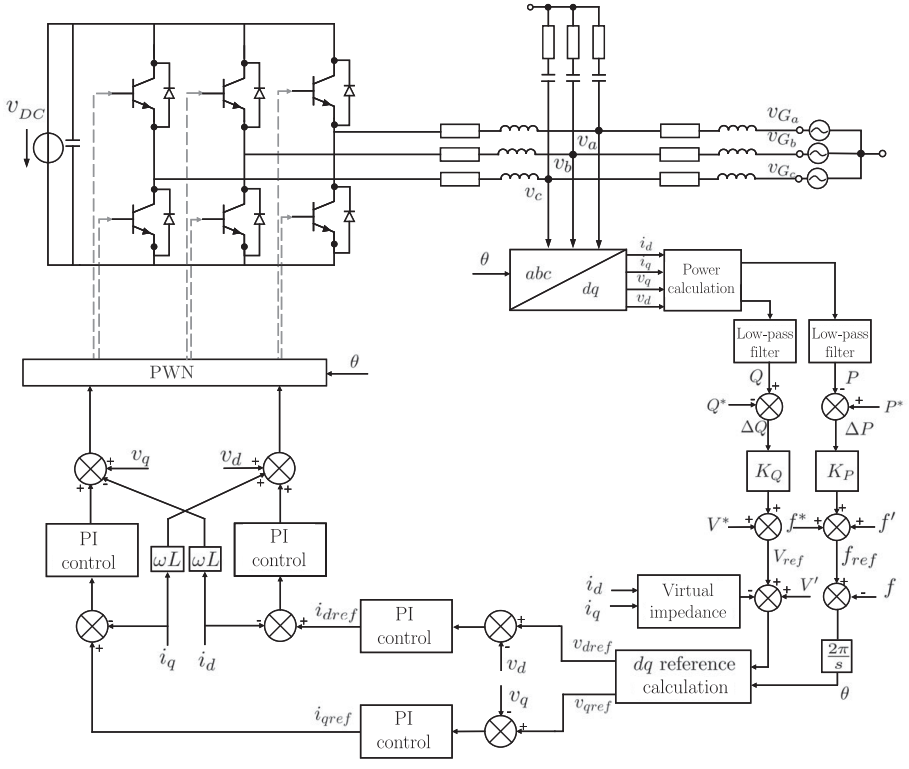

Figure 2.5 A typical droop control scheme implemented on a three-phase inverter.

the current references for the inner loop (see Figure 2.5). It should be noted that the droop control expressed in (2.2) is based on a heuristic correlation between $P - f$ and $Q - V$ under the assumption of an inductively dominant grid (backbone feeders with small R/X ratios). For microgrids where the inductive assumption no longer holds, however, the standard droop control in (2.2) may need to be modified to enable better performances [6, 16, 28]. Furthermore, the droop control can also include a virtual impedance loop (see Figure 2.5) to achieve extra desirable properties. Readers are referred to references such as [5, 29] for details.

The *secondary control* aims to fully restore the microgrid's voltage and frequency by eliminating the remaining deviations after the droop control is applied. To achieve the secondary control, the microgrid's frequency and the terminal voltage of a DER participating in the secondary control are compared with the reference frequency and voltage amplitude f^* and V^*, respectively [30]. The error signals are regulated through the secondary controller to generate secondary control signals as follows:

$$f' = K_{Pf}(f^* - f) + K_{If}\int(f^* - f) + \Delta f_s \tag{2.3a}$$

$$V' = K_{PV}(V^* - V) + K_{IV}\int(V^* - V), \tag{2.3b}$$

https://doi.org/10.1017/9781108596589.004 Published online by Cambridge University Press

where K_{Pf}, K_{If}, K_{PV}, and K_{IV} are the secondary control parameters, and Δf_s is a synchronization term that facilitates the microgrid's synchronization with the main grid. When the microgrid is islanded, Δf_s is always zero.

As can be seen in Figure 2.5, signals f' and V' are then added to the droop control to push the droop characteristics of each DER up or down to restore the frequency and the voltage to their nominal values. The secondary control in (2.3) can be implemented by a centralized controller or by a distributed controller through distributed averaging techniques [31].

2.2.3 Master–Slave Control

An islanded microgrid can also adopt the so-called master–slave control [11], where a leader DER or an energy storage unit operates in the grid-forming mode to provide voltage and frequency references for the microgrid (V/f control) while the rest of the DERs operate in the grid-following mode (PQ control) [27]. The "master" DER, therefore, should have sufficient capacity to absorb load variations during islanded operations. A typical V/f control scheme and a typical PG control scheme deployed on a two-level, three-phase inverter are illustrated in Figures 2.6 and 2.7, respectively.

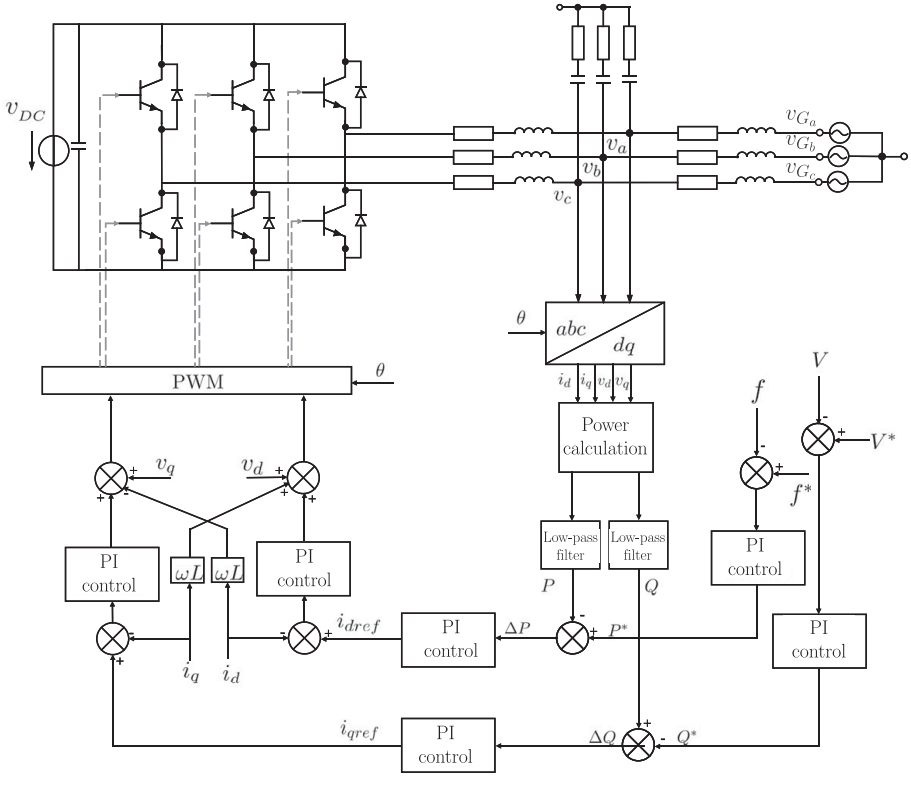

Figure 2.6 A typical V/f scheme for microgrid inverter.

https://doi.org/10.1017/9781108596589.004 Published online by Cambridge University Press

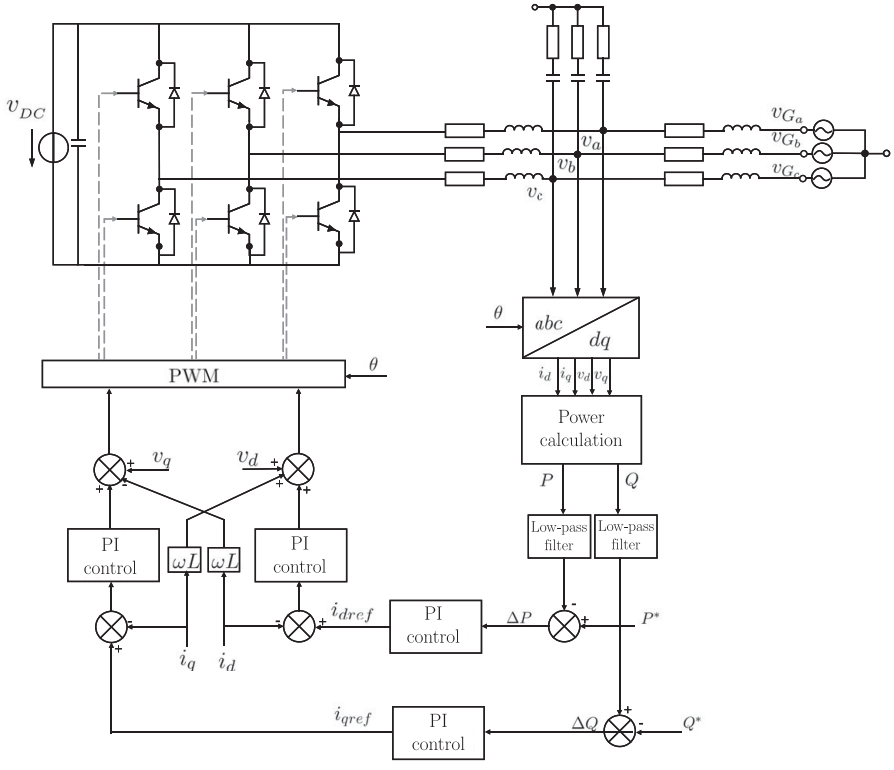

Figure 2.7 A typical PQ control scheme for microgrid inverter.

For the V/f control in Figure 2.6, the inner current-controlled loop can be similar to that described in Subsection 2.2.2. The outer loop aims to provide reference frequency and voltage amplitude at the DER's coupling point, somehow emulating the behavior of a slack bus. Measured frequency f is compared with its reference f_{ref}, and the error is regulated by a PI controller to provide reference signal P_{ref} for active power. Measured voltage V is compared with its reference V_{ref}, and the error is regulated by a PI controller to provide reference signal Q_{ref} for reactive power [27]. The two references are then used to generate reference signals for the inner loop. As a result, a DER's V/f control will shift its active and reactive power in such a way that its terminal voltage and frequency will remain relatively constant.

A major difference between the PQ control in Figure 2.7 and a grid-forming control is that the outer loop of the PQ control is a power control instead of a voltage-controlled one. A DER's active and reactive power outputs can be calculated, filtered, and then compared with their reference values (see Figure 2.7). The errors in power outputs are then regulated through a PI controller to obtain current references i_{dref} and i_{qref}, which will be the input signals for the inner control loop. The inner current-controlled loop for the PQ control can be similar to the one described in Subsection 2.2.2. In addition to the aforementioned standard PQ control scheme, many variations can be derived to achieve effective or simplified PQ control for different use cases.

https://doi.org/10.1017/9781108596589.004 Published online by Cambridge University Press

2.2.4 Tertiary Control and Remedial Action Schemes

Tertiary Control. Tertiary control can be used to achieve longer-term, high-level objectives defined by microgrids and the main grid. For instance, reliably and efficiently operating a microgrid in the long term can be ensured by the optimal power flow [32]. The OPF control aims to minimize some objectives such as the microgrid's operational cost, unreliability cost, and environmental cost by optimally dispatching DERs, reactive power resources, transformer tap changer settings, demand response resources, and even droop coefficients. OPF can be performed by a microgrid EMS or in a distributed way that may involve other advanced functionalities such as electricity price forecasting, state estimation, or storage state of charge estimation. Once OPF is solved, the results can be sent to the secondary and primary controllers as set points that can be executed locally.

Microgrid Remedial Action Scheme (microRAS). The remedial action scheme, often referred to as fast load shedding, is used to mitigate highly disastrous events that cannot be covered by primary or secondary controls [33, 34]. Specifically, when a microgrid lacks generation and battery power to restore its frequency to an acceptable range, microRAS will be triggered to shed some of the load. In this situation, if the time required to shed the load is long, the condition will continue to deteriorate and will cause more of the load to be shed, which can lead to system collapse. Thus, it is desirable to have a fast microRAS that sheds the minimum amount of load to maintain system stability. microRAS needs to identify an actual island, calculate the load flow in all relevant parts of the microgrid, and compare the load with the available electrical power inside the island. As soon as a shortage is detected, the load shedding system starts operating and sheds the load that cannot be served. To minimize the amount of load to be shed, the microgrid's EMS can solve a mixed-integer programming (MIP) problem based on real-time information gathered from the microgrid's various components. The amount that needs to be shed will then be communicated to the load. The advantage of microRAS over the traditional frequency-relay-based load shedding is that it responds faster, sheds less load, and leads to minimum outages for electricity users.

2.3 Virtual Synchronous Generator

Among many other microgrid control approaches, the virtual synchronous generator (VSG) is a control scheme that aims to make the inverters emulate the behavior of a synchronous generator as closely as possible [35–37]. The upper part of Figure 2.8 shows the inverter circuits that mimic the energy conversion process of a synchronous machine, where the inductance L_s and the resistance r_s are used to emulate the stator winds of the synchronous machine. The control system for the inverter is designed to produce the reference back electromotive force (EMF) of a synchronous generator such that the following synchronous machine equations can be emulated:

$$\mathbf{v}_{abc} = -r_s \mathbf{i}_{abc} - L_s \frac{d\mathbf{i}_{abc}}{dt} + \mathbf{e}_{abc} \tag{2.4}$$

https://doi.org/10.1017/9781108596589.004 Published online by Cambridge University Press

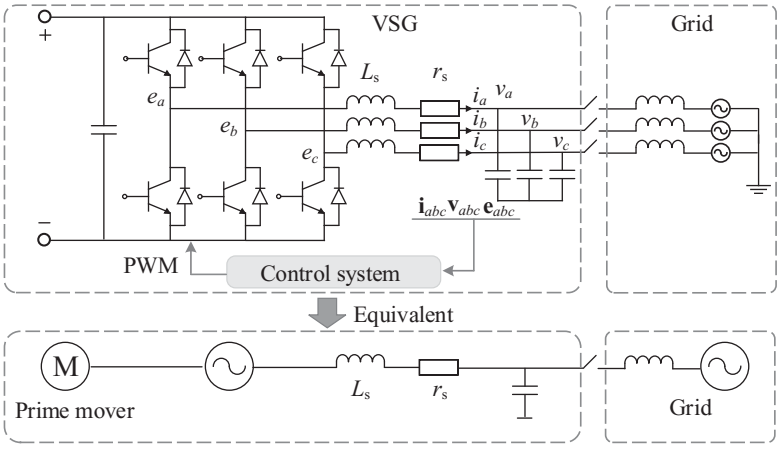

Figure 2.8 Structure of VSG.

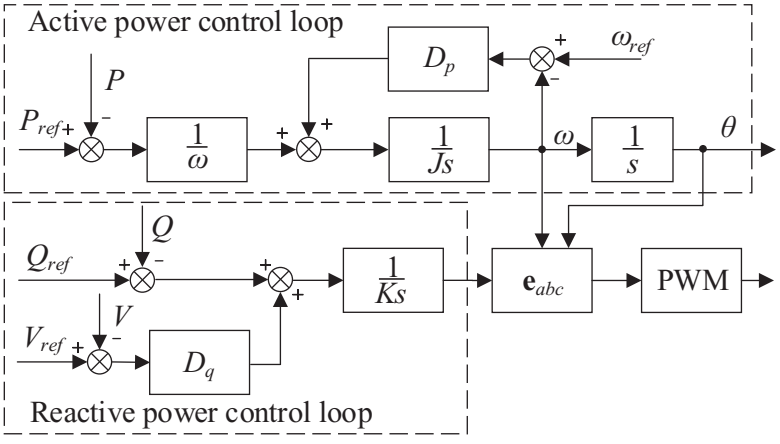

Figure 2.9 Control scheme of VSG.

where $\mathbf{u}_{abc} = [u_a, u_b, u_c]^T$, $\mathbf{i}_{abc} = [i_a, i_b, i_c]^T$ and $\mathbf{e}_{abc} = [e_a, e_b, e_c]^T$ are the generator terminal voltages, currents, and the back EMF, respectively. As shown in Figure 2.9, the VSG control system consists of an active power control loop and a reactive power control loop. The former mimics the behavior of the rotor and speed governor, while the latter mimics the excitation system of a synchronous machine. The back EMF is determined by both the active and reactive power control loops. For a round rotor machine with a constant excitation current, the back EMF can be evaluated by

$$\mathbf{e}_{abc} = M_f i_f \frac{d\theta}{dt}\mathbf{A} \tag{2.5}$$

where M_f is the mutual inductance between the rotor and the stator, i_f is the rotor excitation current, θ is the rotor angle, and $\mathbf{A}= [sin\theta, sin(\theta - \frac{2\pi}{3}), sin(\theta - \frac{4\pi}{3})]^T$.

https://doi.org/10.1017/9781108596589.004 Published online by Cambridge University Press

The active power control loop produces rotor swing equations including the speed-active power droop effect. The rotor swing equation with frequency-active power droop control can be expressed as

$$\begin{cases} J\frac{d\omega}{dt} = T_m - T_e - D_p(\omega - \omega_{ref}) \\ \frac{d\theta}{dt} = \omega \end{cases} \tag{2.6}$$

where J is the moment of inertia; T_m and T_e are the mechanical and electrical torque, respectively; D_p is the damping factor; ω is the angular speed; and ω_{ref} is its nominal value. By mimicking the rotor swing equations, VSG could provide digitized inertia and damping.

In the reactive power control loop, the voltage-reactive power droop is considered to regulate reactive power according to the deviation between voltage amplitude ΔV and reactive power difference ΔQ. The voltage-drooping coefficient D_q is selected to represent the reactive power change with respect to the voltage changes, i.e. $D_q = -\Delta Q/\Delta V$. Then, this error is added into the tracking error between Q_{ref} and Q to generate $M_f i_f$. Finally, the reference back EMF of VSG can be generated as shown in Figure 2.9.

VSG is still being studied to investigate its capabilities for providing inertia and damping. Various control schemes for VSG have been proposed for potential use cases including the following: damping the DC-side fluctuation in a multiterminal direct current (MTDC) system [38], improving the power transfer capabilities of a weak AC grid [39], and providing VSG functionalities for an interface converter in an islanded hybrid AC/DC microgrid [40]. Recently, a stability analysis has been performed for VSG including the small-signal stability of a power grid with VSG [41], and a parameter optimization has been proposed that aims to improve VSG performance in microgrids [42].

2.4 A Note about DER Modeling

In recent years, several studies have been published that aim to guide readers through the various facets of DER modeling, analysis, and simulation. Hence, instead of covering the detailed modeling of DERs, this chapter will list a few working resources for the modeling of DER units and control:

- General guide to generators and machine modeling:
  - *Power System Stability and Control* [17]
  - *Analysis of Electric Machinery and Drive Systems* [43]
- General guide to DER modeling:
  - *Simulation of Power System with Renewables* [44]

https://doi.org/10.1017/9781108596589.004 Published online by Cambridge University Press

- Photovoltaic power system modeling:
  - *Photovoltaic Power System: Modeling, Design, and Control* [45]
- Wind turbine power system modeling:
  - *Power Conversion and Control of Wind Energy Systems* [46]
- Energy storage system modeling:
  - *Converter-Interfaced Energy Storage Systems: Context, Modelling and Dynamic Analysis* [47]
- Fuel cell modeling:
  - *Modeling and Control of Fuel Cells: Distributed Generation Applications* [48]

References

[1] G. O. Suvire, M. G. Molina, and P. E. Mercado, "Improving the Integration of Wind Power Generation into AC Microgrids Using Flywheel Energy Storage," *IEEE Transactions on Smart Grid*, vol. 3, no. 4, pp. 1945–1954, 2012.

[2] A. Chaouachi, R. M. Kamel, R. Andoulsi, and K. Nagasaka, "Multiobjective Intelligent Energy Management for a Microgrid," *IEEE Transactions on Industrial Electronics*, vol. 60, no. 4, pp. 1688–1699, 2013.

[3] F. R. Yu, P. Zhang, W. Xiao, and P. Choudhury, "Communication Systems for Grid Integration of Renewable Energy Resources," *IEEE Network*, vol. 25, no. 5, pp. 22–29, 2011.

[4] Z. Fan, P. Kulkarni, S. Gormus, C. Efthymiou, G. Kalogridis, M. Sooriyabandara, Z. Zhu, S. Lambotharan, and W. H. Chin, "Smart Grid Communications: Overview of Research Challenges, Solutions, and Standardization Activities," *IEEE Communications Surveys & Tutorials*, vol. 15, no. 1, pp. 21–38, 2013.

[5] J. M. Guerrero, M. Chandorkar, T.-L. Lee, and P. C. Loh, "Advanced Control Architectures for Intelligent Microgrids – Part I: Decentralized and Hierarchical Control," *IEEE Transactions on Industrial Electronics*, vol. 60, no. 4, pp. 1254–1262, 2013.

[6] J. M. Guerrero, L. G. de Vicuña, J. Matas, M. Castilla, and J. Miret, "Output impedance Design of Parallel-Connected UPS Inverters with Wireless Load-Sharing Control," *IEEE Transactions on Industrial Electronics*, vol. 52, no. 4, pp. 1126–1135, 2005.

[7] M. Castilla, L. G. De Vicuña, J. Guerrero, J. Matas, and J. Miret, "Design of Voltage-Mode Hysteretic Controllers for Synchronous Buck Converters Supplying Microprocessor Loads," *IEE Proceedings–Electric Power Applications*, vol. 152, no. 5, pp. 1171–1178, 2005.

[8] H. Han, X. Hou, J. Yang, J. Wu, M. Su, and J. M. Guerrero, "Review of Power Sharing Control Strategies for Islanding Operation of AC Microgrids," *IEEE Transactions on Smart Grid*, vol. 7, no. 1, pp. 200–215, 2016.

[9] J. M. Guerrero, J. Matas, L. G. de Vicuña, M. Castilla, and J. Miret, "Wireless-Control Strategy for Parallel Operation of Distributed-Generation Inverters," *IEEE Transactions on Industrial Electronics*, vol. 53, no. 5, pp. 1461–1470, 2006.

https://doi.org/10.1017/9781108596589.004 Published online by Cambridge University Press

[10] J. M. Guerrero, L. G. de Vicuña, J. Matas, M. Castilla, and J. Miret, "A Wireless Controller to Enhance Dynamic Performance of Parallel Inverters in Distributed Generation Systems," *IEEE Transactions on Power Electronics*, vol. 19, no. 5, pp. 1205–1213, 2004.

[11] J. M. Guerrero, L. Hang, and J. Uceda, "Control of Distributed Uninterruptible Power Supply Systems," *IEEE Transactions on Industrial Electronics*, vol. 55, no. 8, pp. 2845–2859, 2008.

[12] J. M. Guerrero, N. Berbel, J. Matas, J. L. Sosa, and L. G. de Vicuña, "Control of Line-Interactive UPS Connected in Parallel Forming a Microgrid," in *2007 IEEE International Symposium on Industrial Electronics*, pp. 2667–2672, 2007.

[13] M. Castilla, L. G. de Vicuña, J. M. Guerrero, J. Miret, and N. Berbel, "Simple Low-Cost Hysteretic Controller for Single-Phase Synchronous Buck Converters," *IEEE Transactions on Power Electronics*, vol. 22, no. 4, pp. 1232–1241, 2007.

[14] M. Castilla, L. G. de Vicuña, J. M. Guerrero, J. Matas, and J. Miret, "Designing VRM Hysteretic Controllers for Optimal Transient Response," *IEEE Transactions on Industrial Electronics*, vol. 54, no. 3, pp. 1726–1738, 2007.

[15] J. C. Vasquez, R. A. Mastromauro, J. M. Guerrero, and M. Liserre, "Voltage Support Provided by a Droop-Controlled Multifunctional Inverter," *IEEE Transactions on Industrial Electronics*, vol. 56, no. 11, pp. 4510–4519, 2009.

[16] J. M. Guerrero, J. Matas, L. G. de Vicuña, M. Castilla, and J. Miret, "Decentralized Control for Parallel Operation of Distributed Generation Inverters Using Resistive Output Impedance," *IEEE Transactions on Industrial Electronics*, vol. 54, no. 2, pp. 994–1004, 2007.

[17] P. Kundur, *Power System Stability and Control*. McGraw-Hill, 1994.

[18] J. Machowski, J. Bialek, and J. Bumby, *Power System Dynamics: Stability and Control*. John Wiley & Sons, 2011.

[19] J. M. Guerrero, P. C. Loh, T.-L. Lee, and M. Chandorkar, "Advanced Control Architectures for Intelligent Microgrids – Part II: Power Quality, Energy Storage, and AC/DC Microgrids," *IEEE Transactions on Industrial Electronics*, vol. 60, no. 4, pp. 1263–1270, 2013.

[20] J. Schiffer, "Stability and Power Sharing in Microgrids," Ph.D. dissertation, 2015.

[21] A. J. Wood, B. F. Wollenberg, and G. B. Sheblé, *Power Generation, Operation, and Control*. John Wiley & Sons, 2013.

[22] H. W. Dommel, *Notes on Power System Analysis*. University of British Columbia, 1975.

[23] H. D. Vu and J. Agee, "WECC Tutorial on Speed Governors," WECC Control Work Group, 1998.

[24] Y. Li, P. Zhang, L. Ren, and T. Orekan, "A Geršgorin Theory for Robust Microgrid Stability Analysis," in *2016 IEEE Power and Energy Society General Meeting (PESGM)*. IEEE, pp. 1–5, 2016.

[25] A. Engler, "Applicability of Droops in Low Voltage Grids," *International Journal of Distributed Energy Resources*, vol. 1, no. 1, pp. 1–6, 2005.

[26] F. Katiraei, R. Iravani, N. Hatziargyriou, and A. Dimeas, "Microgrids Management," *IEEE Power and Energy Magazine*, vol. 6, no. 3, pp. 54–65, 2008.

[27] C. Wang, J. Wu, J. Ekanayake, and N. Jenkins, *Smart Electricity Distribution Networks*. CRC Press, 2017.

[28] K. De Brabandere, B. Bolsens, J. Van den Keybus, A. Woyte, J. Driesen, R. Belmans, and K. Leuven, "A Voltage and Frequency Droop Control Method for Parallel Inverters,"

in *2004 IEEE 35th Annual Power Electronics Specialists Conference (IEEE Cat. No. 04CH37551)*, vol. 4. IEEE, pp. 2501–2507, 2004.

[29] J. M. Guerrero, J. C. Vasquez, J. Matas, L. G. de Vicuña, and M. Castilla, "Hierarchical Control of Droop-Controlled AC and DC Microgrids – a General Approach toward Standardization," *IEEE Transactions on Industrial Electronics*, vol. 58, no. 1, pp. 158–172, 2011.

[30] A. Bidram and A. Davoudi, "Hierarchical Structure of Microgrids Control System," *IEEE Transactions on Smart Grid*, vol. 3, no. 4, pp. 1963–1976, 2012.

[31] J. W. Simpson-Porco, Q. Shafiee, F. Dörfler, J. C. Vasquez, J. M. Guerrero, and F. Bullo, "Secondary Frequency and Voltage Control of Islanded Microgrids via Distributed Averaging," *IEEE Transactions on Industrial Electronics*, vol. 62, no. 11, pp. 7025–7038, 2015.

[32] Y. Levron, J. M. Guerrero, and Y. Beck, "Optimal Power Flow in Microgrids with Energy Storage," *IEEE Transactions on Power Systems*, vol. 28, no. 3, pp. 3226–3234, 2013.

[33] C. Gouveia, J. Moreira, C. Moreira, and J. P. Lopes, "Coordinating Storage and Demand Response for Microgrid Emergency Operation," *IEEE Transactions on Smart Grid*, vol. 4, no. 4, pp. 1898–1908, 2013.

[34] Y.-Y. Hong, M.-C. Hsiao, Y.-R. Chang, Y.-D. Lee, and H.-C. Huang, "Multiscenario Underfrequency Load Shedding in a Microgrid Consisting of Intermittent Renewables," *IEEE Transactions on Power Delivery*, vol. 28, no. 3, pp. 1610–1617, 2013.

[35] Q.-C. Zhong and G. Weiss, "Synchronverters: Inverters That Mimic Synchronous Generators," *IEEE Transactions on Industrial Electronics*, vol. 58, no. 4, pp. 1259–1267, 2011.

[36] H.-P. Beck and R. Hesse, "Virtual Synchronous Machine," in *2007 9th International Conference on Electrical Power Quality and Utilisation*. IEEE, pp. 1–6, 2007.

[37] K. Visscher and S. W. H. De Haan, "Virtual Synchronous Machines (VSG's) for Frequency Stabilisation in Future Grids with a Significant Share of Decentralized Generation," in *CIRED Seminar 2008: SmartGrids for Distribution*. IET, pp. 1–4, 2008.

[38] C. Li, Y. Li, Y. Cao, H. Zhu, C. Rehtanz, and U. Häger, "Virtual Synchronous Generator Control for Damping DC-Side Resonance of VSC-MTDC System," *IEEE Journal of Emerging and Selected Topics in Power Electronics*, vol. 6, no. 3, pp. 1054–1064, 2018.

[39] A. Asrari, M. Mustafa, M. Ansari, and J. Khazaei, "Impedance Analysis of Virtual Synchronous Generator-Based Vector Controlled Converters for Weak AC Grid Integration," *IEEE Transactions on Sustainable Energy*, vol. 10, no. 3, pp. 1481–1490, 2019.

[40] G. Melath, S. Rangarajan, and V. Agarwal, "A Novel Control Scheme for Enhancing the Transient Performance of an Islanded Hybrid AC-DC Microgrid," *IEEE Transactions on Power Electronics*, vol. 34, no. 10, pp. 9644–9654, 2019.

[41] W. Du, Q. Fu, and H. Wang, "Power System Small-Signal Angular Stability Affected by Virtual Synchronous Generators," *IEEE Transactions on Power Systems*, 2019.

[42] J. Alipoor, Y. Miura, and T. Ise, "Stability Assessment and Optimization Methods for Microgrid with Multiple VSG Units," *IEEE Transactions on Smart Grid*, vol. 9, no. 2, pp. 1462–1471, 2018.

[43] P. C. Krause, O. Wasynczuk, S. D. Sudhoff, and S. Pekarek, *Analysis of Electric Machinery and Drive Systems*. Wiley-IEEE Press, 2002, vol. 2.

[44] L. Kunjumuhammed, S. Kuenzel, and B. Pal, *Simulation of Power System with Renewables*. Academic Press, 2019.

[45] W. Xiao, *Photovoltaic Power System: Modeling, Design, and Control*. John Wiley & Sons, 2017.
[46] B. Wu, Y. Lang, N. Zargari, and S. Kouro, *Power Conversion and Control of Wind Energy Systems*. John Wiley & Sons, 2011, vol. 76.
[47] F. Milano and Á. O. Manjavacas, *Converter-Interfaced Energy Storage Systems: Context, Modelling and Dynamic Analysis*. Cambridge University Press, 2019.
[48] M. H. Nehrir and C. Wang, *Modeling and Control of Fuel Cells: Distributed Generation Applications*. John Wiley & Sons, 2009, vol. 41.

https://doi.org/10.1017/9781108596589.004 Published online by Cambridge University Press